Acta Crystallographica Section A
Foundations of Crystallography
ISSN 0108-7673

Received 22 December 2000
Accepted 6 February 2001

Critical examination of the radial functions in the Hansen–Coppens multipole model through topological analysis of primary and refined theoretical densities

Anatoliy Volkov and Philip Coppens*

Department of Chemistry, State University of New York at Buffalo, Buffalo, NY 14260-3000, USA. Correspondence e-mail: coppens@acsu.buffalo.edu

A double-zeta (DZ) multipolar model has been applied to theoretical structure factors of four organic molecular crystals as a test of the ability of the multipole model to faithfully retrieve a theoretical charge density. The DZ model leads to significant improvement in the agreement with the theoretical charge density along the covalent bonds and its topological parameters, and eliminates some of the bias introduced by the limited flexibility of the radial functions when a theoretical density is projected into the conventional multipole formalism. The DZ model may be too detailed for analysis of experimental data sets of the accuracy and resolution typically achieved at present, but provides guidance for the type of algorithms to be adapted in future studies.

1. Introduction

In previous studies (Volkov, Abramov *et al.*, 2000; Volkov, Gatti *et al.*, 2000), we have analyzed the effect of the experimental multipole model on the theoretical crystal charge density when the latter is projected into the multipole functions by refinement of theoretical static structure factors. The effect of the projection was examined through topological analysis (Bader, 1990) of both the density derived directly from the wavefunction (the 'primary' density) and the density from the multipole model. The topological properties examined were net atomic charges, net atomic volumes, molecular dipole moments and the properties of charge density at bond critical points.

Our analysis was limited to the Coppens–Hansen formalism (Hansen & Coppens, 1978; Coppens, 1997) with n in the factor r^n of the deformation radial functions $R(r)$ for dipoles, quadrupoles and octupoles equal to 2, 2 and 3 for first-row atoms and 1, 2 and 3 for H atoms, respectively.

The main conclusions were:

(i) The experimental multipole model introduces a bias in the charge density, which is similar for Hartree–Fock (HF) and density functional (DFT) densities.

(ii) Experimental charge densities tend to agree more closely with theoretical DFT than with HF densities.

Although our calculations were limited to the use of the atomic orbital (AO) representation of the Bloch functions, in which each AO is described by a linear combination of Gaussian-type functions, subsequent studies (Volkov, Blaha *et al.*, 2001) showed a similar bias in refinement of theoretical structure factors obtained from full-potential linearized-augmented-plane-wave (FP-LAPW) DFT calculations using the *WIEN97* program, thus ruling out the use of Gaussian-type functions in theoretical calculations as a potential source of the differences.

The inability of the limited multipole expansion to accurately reproduce the topological parameters of the primary densities illustrates the need for a critical examination of the model. What changes in the algorithm can lead to a more faithful reproduction of the primary density?

Several authors have noted that the main shortcoming of the model originates in the restricted nature of the radial functions (Swaminathan *et al.*, 1984), which usually correspond to a minimal basis set, with a single function for each value of the angular-momentum number l (Chandler *et al.*, 1980; Chandler & Spackman, 1982). In the latter papers, based on refinements of simple diatomic molecules, several recipes were suggested to improve the flexibility of the radial functions. These include separate optimization of all valence exponents for each radial function and the use of several (up to four) sets of multipolar functions for each pseudoatom. Benchmark refinements for an H_2 molecule showed that an acceptable fit to a number of physical properties can be obtained if either all exponents are optimized separately for all single-term radial functions or two-term functions are used (Chandler *et al.*, 1980). For first-row diatomic hydrides, however, it was important to include sharp core polarization functions into the pseudoatom basis, as well as an additional monopole function with exponent intermediate between that of a core and a valence function (Chandler & Spackman,

1982), but no further improvements were observed upon the use of two-term functions.

A similar approach was used in the 9 K experimental charge-density analysis of *trans*-tetraaminedinitronickel(II) (Iversen *et al.*, 1997). Introduction of two sets of multipolar functions for the Ni atom and separate optimization of all exponents of the radial functions of the nitrite nitrogen atoms greatly improved the agreement between experiment and theory for the charge densities and the Laplacians at the bond critical points.

It is evident that the use of several sets of multipolar functions for each pseudoatom expansion has promise, but requires more detailed analysis and testing. Here we describe the testing of a 'double zeta' (DZ) multipolar formalism (two sets of deformation functions for each pseudoatom), using model densities from *ab initio* periodic Hartree–Fock (PHF) and periodic density functional (PDFT) calculations. Topological parameters and agreement factors for the density along the bond paths are used in the assessment of basis-set adequacy.

2. Crystal data

Theoretical results on *p*-nitroaniline [$C_6H_6N_2O_2$ (PNA)], methyl carbamate [$C_2H_5NO_2$ (MC)], carbonohydrazide [$(NH_2NH)_2CO$ (CH)] and γ-aminobutyric acid [$C_4H_9NO_2$ (GABA)] were used for this study

Structural parameters for *p*-nitroaniline [space group $P2_1/n$, Fig. 1(*a*)] are from the multipole refinement of high-quality 20 K synchrotron data (Volkov, Abramov *et al.*, 2000; Volkov, Gatti *et al.*, 2000). The crystal structure contains sheets of N—O···H—N hydrogen-bonded molecules, oriented perpendicular to the [101] direction, with each molecule being hydrogen-bonded to four other molecules. Methyl carbamate parameters are from a conventional spherical-atom refinement of 123 K X-ray data (Sepehrnia *et al.*, 1987). The crystal structure [space group $P\bar{1}$ (Fig. 1*b*)] consists of almost planar methyl carbamate molecules, arranged into planar layers parallel to $(01\bar{2})$ by NH···O and CH···O hydrogen bonds. To compensate for the shortening of X-ray-determined X—H bonds, H atoms in PNA and MC were placed at 1.066 and 1.08 Å from C along the C_{methyl}—H and $C_{aromatic}$—H, and at 1.01 Å from N along N—H bonds, which correspond to the averaged distances in X—C—H_3, $C_{aromatic}$—H and X_2—N—H groups, respectively (*International Tables for Crystallography*, 1992).

Structural parameters for carbonohydrazide [space group $P2_1/c$ (Fig. 1*c*)] were taken from refinement of the accurate 15 K single-crystal neutron diffraction data (Jeffrey *et al.*, 1985). This crystal structure exhibits extensive hydrogen-bonding interactions. The crystals contain three distinct types of hydrogen-bonded dimers which are stacked along the *a* axis. Information on γ-aminobutyric acid [space group $P2_1/a$ (Fig. 1*d*)] was obtained from the refinement of accurate neutron data collected at 122 K and corrected for anisotropy in atomic and molecular vibrations (Weber *et al.*, 1983). In the crystal structure GABA, zwitterions are arranged in sheets parallel to (001), with non-polar trimethylene groups near $z = 0$ and the polar groups near $z = \frac{1}{2}$. The sheets are cross-linked by a three-dimensional network of strong N—H···O hydrogen bonds.

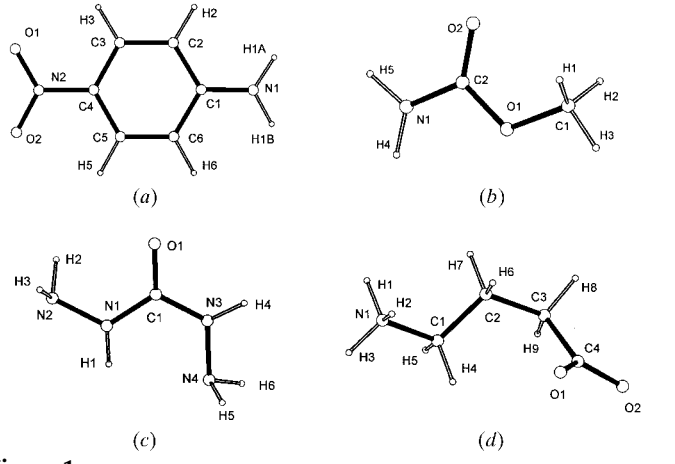

Figure 1
Molecular structures of (*a*) *p*-nitroaniline, (*b*) methyl carbamate, (*c*) carbonohydrazide and (*d*) γ-aminobutyric acid.

3. Computational details

3.1. *Ab initio* calculations

Fully periodic (crystal) calculations were performed with the *CRYSTAL98* package (Saunders *et al.*, 1998) at HF (PHF) and DFT (PDFT) levels. DFT calculations for PNA were performed using Becke's (1988) functional, which includes Slater exchange along with corrections involving the gradient of the density, combined with Perdew and Wang's gradient-corrected correlation functional (BPW91) (Perdew & Wang, 1992). For MC, CH and GABA, Becke's three-parameter hybrid exchange (Becke, 1993) was combined with the non-local correlation functional of Lee, Yang & Parr (Lee *et al.*, 1988) (B3LYP). All periodic calculations employed the split-valence 6-31G** basis set (Hariharan & Pople, 1973), which was modified in the PNA calculations as described in a previous paper (Abramov *et al.*, 2000), but was left unmodified for MC, CH and GABA. The shrinking factor for the Monkhorst net (Monkhorst & Pack, 1976) was set equal to 8 for all compounds, which produced 260 **k** points in the irreducible part of the *Brillouin zone* in PNA and 170 **k** points in MC, CH and GABA. Analysis of charge densities was performed with *TOPOND98* (Gatti, 1999).

Single-molecule calculations for all compounds were performed at HF, DFT (B3LYP) and second-order Møller–Plesset perturbation (Møller & Plesset, 1934) (MP2) levels of theory with the *GAUSSIAN94* program (Frisch *et al.*, 1995). The standard molecular split-valence 6-311G** and 6-311++G** basis sets (Krishnan *et al.*, 1980; Clark *et al.*, 1983) were used. In all single-molecule calculations, the crystal molecular geometries were used.

Table 1
Effect of the SZ multipole model with two different n_l combinations on the properties of the PHF/6-31G** crystal density at the BCP's in the PNA molecule.

				Hessian eigenvalues (e Å^{-5})			
	Δ_{BCP} (Å)†	ρ (eÅ^{-3})	$\nabla^2\rho$ (eÅ^{-5})	λ_1	λ_2	λ_3	ε
Average O—N							
Primary‡	0.013	3.35	−26.7	−30.3	−27.1	30.7	0.12
$n_{1\ldots3}$ = 2, 2, 3	0.001	3.26	−13.8	−27.6	−25.7	39.7	0.10
$n_{1\ldots3}$ = 4, 4, 6	0.009	3.27	−22.0	−27.6	−25.3	29.9	0.10
N_{amino}—C							
Primary	0.228	2.20	−21.9	−17.6	−17.3	13.2	0.02
$n_{1\ldots3}$ = 2, 2, 3	0.132	2.18	−24.6	−17.3	−15.3	7.9	0.13
$n_{1\ldots3}$ = 4, 4, 6	0.221	2.18	−20.6	−15.5	−14.0	8.8	0.11
N_{nitro}—C							
Primary	0.271	1.77	−4.8	−12.4	−9.8	17.4	0.27
$n_{1\ldots3}$ = 2, 2, 3	0.235	1.72	−10.2	−11.4	−8.5	9.7	0.35
$n_{1\ldots3}$ = 4, 4, 6	0.256	1.72	−1.2	−10.0	−7.9	16.8	0.27
Average C2—C3 and C6—C5							
Primary	0.021	2.18	−23.6	−16.6	−13.0	5.9	0.28
$n_{1\ldots3}$ = 2, 2, 3	0.019	2.16	−20.7	−15.8	−12.7	8.1	0.24
$n_{1\ldots3}$ = 4, 4, 6	0.034	2.19	−23.2	−17.0	−13.0	6.8	0.32
Average N—H							
Primary	0.28	2.34	−46.5	−33.8	−32.0	19.3	0.06
$n_{1\ldots3}$ = 2, 2, 3	0.23	2.25	−28.1	−29.1	−26.7	27.8	0.09
$n_{1\ldots3}$ = 4, 4, 6	0.24	2.30	−37.5	−30.9	−28.7	22.1	0.08
Average C—H							
Primary	0.13	1.99	−27.4	−18.7	−18.0	9.2	0.04
$n_{1\ldots3}$ = 2, 2, 3	0.15	1.93	−21.1	−18.1	−16.9	13.9	0.07
$n_{1\ldots3}$ = 4, 4, 6	0.13	1.97	−25.2	−17.9	−17.1	9.8	0.04

† Δ_{BCP} defines the displacement of the position of the BCP from the bond midpoint. It is defined to be positive when the critical point is displaced towards the second atom. ‡ Primary PHF/6-31G** density.

3.2. Multipole refinements of theoretical structure factors

Theoretical (static) crystal structure factors were obtained through Fourier transform of the ground-state charge density from both PHF and PDFT calculations. In order to simulate a typical X-ray diffraction data set, theoretical structure factors within the range $0 < \sin\theta/\lambda < 1.1$ Å^{-1} were included. All multipole refinements were based on F and carried out with the *XD* package (Koritsanszky *et al.*, 1997) using the Hansen–Coppens (Hansen & Coppens, 1978; Coppens, 1997) multipole formalism. The basic formalism describes the static electron density in the crystal by a superposition of aspherical *pseudoatoms*, the charge density of which is modeled by a nucleus-centered multipole expansion

$$\rho_k(\mathbf{r}) = P_c\rho_c(r) + P_v\kappa^3\rho_v(\kappa r) + \kappa'^3\sum_{l=1}^{4} R_l(\kappa' r)\sum_{m=1}^{l} P_{lm\pm}d_{lm\pm}(\mathbf{r}/r), \quad (1)$$

where ρ_c and ρ_v are spherically averaged free-atom Hartree–Fock core and valence densities normalized to one electron; $d_{lm\pm}$ are real spherical harmonic angular functions; R_l are normalized Slater-type radial functions including a factor r^{n_l}; κ and κ' are dimensionless expansion–contraction parameters, which can be refined in the fitting procedure along with the populations P_v and $P_{lm\pm}$. HF densities are used for the spherically averaged core (ρ_c) and valence (ρ_v) shells. Although in the *ab initio* calculations the crystal density was obtained as a product of atomic Gaussian-type orbitals, in the multipole refinements we used scattering factors derived from Clementi–Roetti atomic functions (Clementi & Roetti, 1974). Stewart has shown that the difference in the radial scattering factors between Clementi orbital products and the corresponding expansion over five Gaussian-type orbitals (basically, the STO-5G basis set) is well under 1% below $\sin\theta/\lambda = 1$ Å^{-1} (Stewart, 1969). Much better agreement should be achieved for split valence basis sets, such as 6-31G**, so the difference in scattering factors should be negligible.

No atomic temperature parameters were refined and all positional parameters were fixed. In order to reduce the number of refined parameters, local-symmetry constraints not higher than m symmetry were applied to some atoms. In all refinements, the multipole expansion was truncated at the octupole level ($l_{max} = 3$). This was justified in previous studies on these and similar compounds, in which changes in topological properties of the charge density upon inclusion of higher multipoles (hexadecapoles) were negligible. A molecular electroneutrality constraint was applied in all refinements. Specific details of individual refinements are discussed below. The program *TOPXD* (Volkov, Abramov *et al.*, 2000) was used for the atoms in molecules (AIM) analysis of the charge densities from the multipole refinement.

4. Results and discussion

4.1. Single-zeta multipole refinements of PHF/6-31G** structure factors of PNA

The normalized radial density function of the deformation functions in the Hansen–Coppens formalism (Hansen & Coppens, 1978; Coppens, 1997) is defined as

$$R_l(r) = \kappa'^3\frac{\zeta^{n_l+3}}{(n_l+2)!}(\kappa' r)^{n_l}\exp(-\kappa'\zeta r), \quad (2)$$

where r is the radial coordinate, ζ is the single Slater exponent, κ' is the expansion–contraction coefficient and the coefficient n_l can be assigned any positive integer number. Energy-optimized single Slater ζ values for electron shells of isolated atoms, calculated by Clementi & Roetti (1974), are fixed, while the κ' parameter is adjusted in the course of the multipole

refinement. Thus the only arbitrary parameter left in the radial density function is the coefficient n_l. Stewart (1976) pointed out that coefficients n_l have to obey the condition $n_l = l$ to ensure a proper solution of Poisson's equation at $r = 0$ for a Coulomb potential. Hansen & Coppens (1978) suggested the use of $n_{1\ldots3} = 2, 2, 3$ for first-row atoms for dipoles ($l = 1$), quadrupoles ($l = 2$) and octupoles ($l = 3$), respectively, based on the relation to the products of atomic orbitals in the quantum-mechanical electron-density formalism. For hydrogen atoms, the n values of 1, 2 are commonly used for $l = 1,2$ (Coppens, 1997). The same method predicts $n_l = 4$ for second-row atoms for all deformation functions. However, for highly accurate *Pendellösung* data on silicon and low-temperature data on NH_4SCN, a better set of deformations functions is obtained when using $n_{1\ldots3} = 4, 4, 6$ (Hansen & Coppens, 1978), while for phosphorous in H_3PO_4 the density functions with $n_{1\ldots3} = 6, 6, 7$ give a superior fit to the experimental data (Moss *et al.*, 1995).

The first two rows for each entry in Table 1 list, respectively, the properties of the charge density at the bond critical points (BCPs) in PNA from a PHF/6-31G** calculation and after multipole refinement of PHF structure factors using the $n_{1\ldots3} = 2, 2, 3$ set for all non-H-atom types. In the latter, only one κ' parameter was refined for all multipoles ($l = 1, \ldots, 3$) for a particular atom. Unlike for simple diatomic molecules (Chandler *et al.*, 1980; Chandler & Spackman, 1982), attempts to refine an independent κ' parameter for each set of multipolar functions produced unstable divergent refinements. The multipole refinement with $n_{1\ldots3} = 2, 2, 3$ will be referred to below as single zeta (SZ), since only a single Slater exponent set of deformation functions is assigned to each atom center.

Table 2
Number of reflections and variables in both PHF/6-31G** and PDFT/6-31G** SZ and DZ multipole refinements of the test compounds.

		SZ		DZ	
Compound	N_{ref}	N_{var}	N_{ref}/N_{var}	N_{var}	N_{ref}/N_{var}
PNA	7241	137	52.9	186	38.9
MC	3984	82	48.6	126	31.6
CH	4240	127	33.4	187	22.7
GABA	6182	136	45.5	223	27.7

To explore if other values lead to superior results, we systematically examined all combinations of n_l between 2, 2, 3 and 8, 8, 8 (a total of 83 combinations) for non-H atoms, *i.e.* the same combination of n_l parameters was tested for C, N and O atoms in each refinement. The n_l values for H atoms were kept at 1, 2 for dipolar and quadrupolar functions, respectively, and all H atoms were assigned a single variable κ' parameter. Surprisingly, judged by the overall agreement of the topological properties with those of the primary density, the best fit was obtained with the 4, 4, 6 deformation set (Table

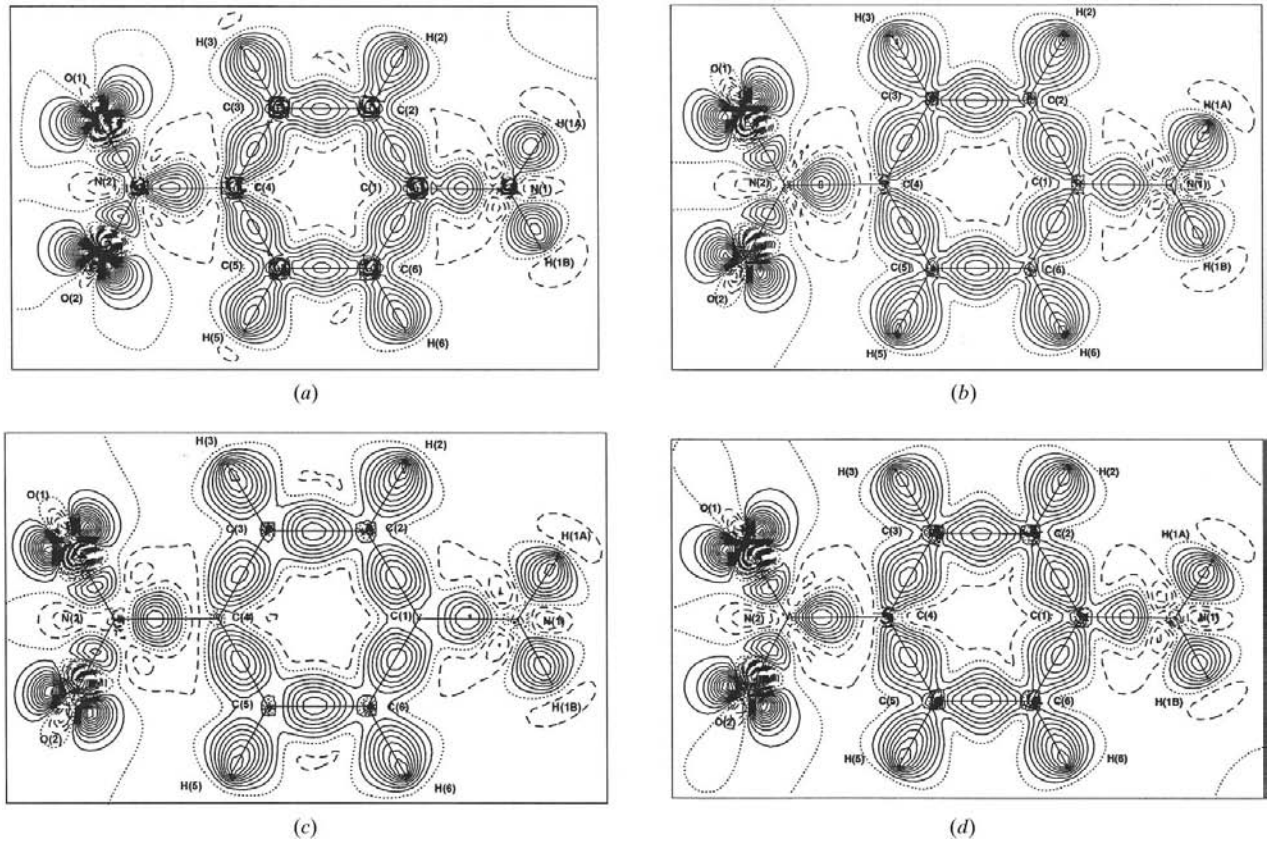

Figure 2
Deformation density in PNA: (*a*) primary density from PHF/6-31G** calculation; (*b*), (*c*) and (*d*) from multipole refinement of PHF/6-31G** structure factors using SZ (2, 2, 3), SZ (4, 4, 6) and DZ models, respectively

Table 3
The n_l combinations that produced the best averaged $R(\rho)$ for all compounds [A—H profiles were excluded from calculation of averaged $R(\rho)$].

	SZ		DZ				
Compound	$R(F)$ (%)	$R(\rho)$ (%) average	$R(F)$ (%)	$R(\rho)$ (%) average	$n_{1\ldots3}$(O)†	$n_{1\ldots3}$(N)†	$n_{1\ldots3}$(C)†
PHF/6-31G**							
PNA	0.68	1.61	0.56	1.06	8	12	14
MC	0.71	2.97	0.54	1.17	8	8	20
CH	0.89	2.93	0.72	1.15	10	12	10
GABA	0.65	2.48	0.56	1.39	10	20	22
PDFT/6-31G**							
PNA	0.80	1.83	0.62	1.11	6	4	8
MC	0.74	2.99	0.56	1.16	10	10	12
CH	0.88	3.05	0.68	1.19	6	16	4
GABA	0.72	2.33	0.63	1.21	8	22	22

† Second deformation set.

1), while the $n_{1\ldots3} = 7, 8, 8$ combination produced the worst fit, indicating that the use of higher values of n_l will not improve the results.

The function described by (2) has a maximum at

$$r_{\max} = n_l/\kappa'\zeta. \tag{3}$$

Analysis of the κ' parameters from refinements with $n_{1\ldots3} = 2, 2, 3$ and 4, 4, 6 sets revealed that, although in the latter case the refined κ' parameters were slightly higher, the increase does not fully compensate for the increase to $n_l = 4$ and 6, so that the maxima of the radial functions are closer to midpoints of the bonds by about 0.1 Å for all C, N and O pseudoatoms. However, examination of the deformation density maps (Fig. 2) shows results from the 4, 4, 6 set to have an unacceptable fit in regions close to atomic cores. Thus, $n_{1\ldots3} = 4, 4, 6$ deformation set produces a much better fit to the electron density near the BCP than the standard 2, 2, 3 set, at the expense of the density fit in the core region. In general, these results support previous observations that the single-ζ radial functions described by (2) are not flexible enough to accurately describe the model density in both the core and the valence regions (Chandler *et al.*, 1980).

4.2. Double-zeta multipole refinements

The use of the single-ζ multipole formalism may be compared with the use of minimal basis sets in quantum-mechanical calculations, though the single-ζ multipole formalism is flexible in the sense that different population parameters are used for each of the spherical harmonic density terms and that higher spherical harmonic terms are included. Extended basis sets are now routinely used in theoretical calculations.

A similar approach may be applied to the multipole model (Chandler *et al.*, 1980; Chandler & Spackman, 1982; Iversen *et al.*, 1997). In the current work, a modification of the program *XD* was used which allows introduction of additional sets of atom-centered spherical harmonic deformation functions with different radial dependence (Koritsanszky, 2000). The values of $n_{1\ldots3} = 2, 2, 3$ are retained for the first deformation set. The second set, used for all non-hydrogen atoms in this study, has a single value of n_l for all l's and a single refinable κ parameter (indicated here as κ'') for each atom type. The basis set for hydrogen atoms has not been extended in this study. The formalism is referred to as double zeta (DZ) throughout this paper.

At the start of each refinement, the initial κ'' value for each particular atom was selected so as to give a maximum of the second deformation function (at $n_l/\kappa''\zeta$) close to the midpoints of the bonds surrounding the atom. To restrict the number of calculations to be performed, all C atoms were assigned identical n_l values for the second deformation set. The number of reflections and number of parameters varied in the SZ and DZ refinements of each of the compounds are listed in Table 2.

To explore the appropriate choice of n_l for the second set of deformation functions, values were varied within a range from 4 to 22 in steps of 2 for each atom type, leading to as many as 1000 different DZ refinements for each of the four compounds, with both HF and DFT structure factors.

Comparison of the properties of the charge density at the BCPs, rather than in a larger volume, is a too restricted criterion for topological similarities between charge densities. As a more general probe, we define an agreement factor $R(\rho)$ for the profile of the charge density along an intramolecular bond as

$$R(\rho) = \sum_{d1}^{d2} |\rho_{\text{primary}} - \rho_{\text{multipole}}| \Big/ \sum_{d1}^{d2} \rho_{\text{primary}}, \tag{4}$$

where ρ_{primary} is the theoretical charge density before multipole refinement and $\rho_{\text{multipole}}$ is the charge density from multipole refinement of the theoretical structure factors. A grid of 101 points along each A–B profile was used, corresponding to a grid spacing slightly larger than 0.01 Å. The parameters $d1$ and $d2$, which define the distance range from the first atom within which the bond-profile factor $R(\rho)$ is calculated, were introduced in order to eliminate the effect of larger contributions from the charge density in the core region. The core-region discrepancies are due to the use of different types of basis functions in the theoretical calculation and the multipole model (Gaussian- and Slater-type functions, respectively). Typical values for $d1$ and $d2$ were 0.2 Å and $d_{A-B} - 0.2$ Å, where d_{A-B} is the bond distance between atoms A and B.

To judge the global fit, an average of the $R(\rho)$ values for the individual profiles is calculated and examined together with the $R(F)$ values, which are a measure of overall fit of the density. The agreement factors and the coefficients giving optimal agreement are listed in Table 3. Both $R(F)$ and $R(\rho)$

are considerably improved by the use of the DZ basis set. While $R(F)$ is also much improved for other combinations of n_l values, the bond-profile R factor $R(\rho)$ is much more sensitive to the choice of the powers of r in the radial functions. The insensitivity of $R(F)$ to changes in the radial model has been noted in earlier studies. (Hansen & Coppens, 1978; Moss *et al.*, 1995; Pérès *et al.*, 1999).

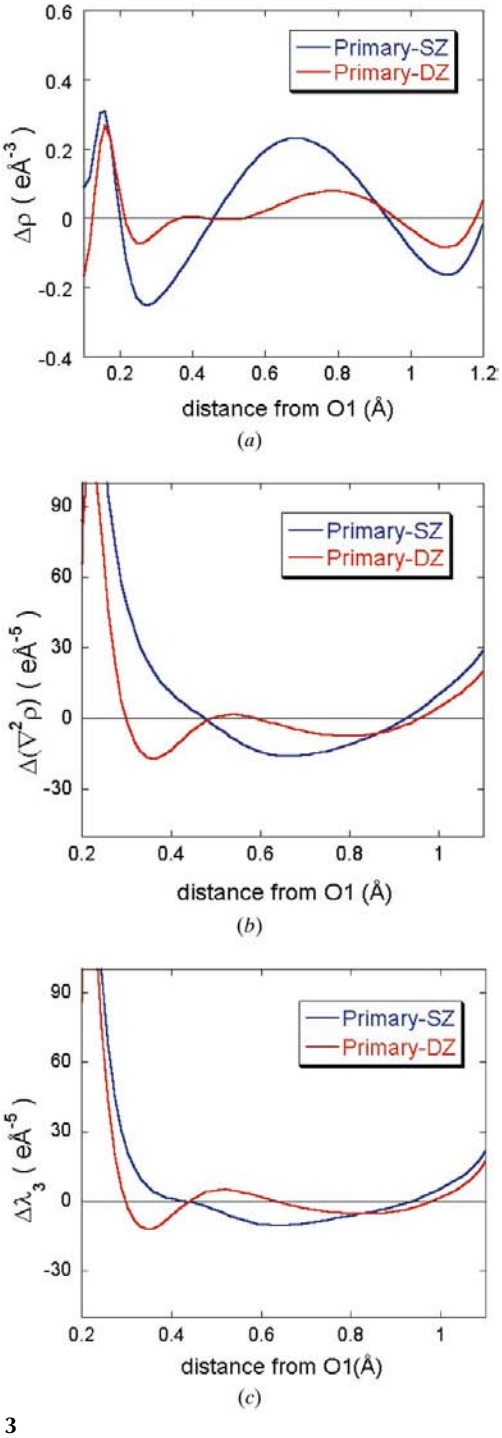

Figure 3
Differences in (*a*) ρ, (*b*) $\nabla^2\rho$ and (*c*) λ_3 profiles along the O1—C1 bond in methyl carbamate for the two models relative to the values based on the original wave function.

The best DZ multipole refinements of PDFT structure factors for individual $A-B$ bond profiles are listed Table 4, together with the corresponding n_l and refined κ' and κ'' values from DZ refinements for both A and B atoms. For comparison, Table 4 also lists the $R(\rho)$ and κ' parameters from the SZ refinements. Without exception, significant improvements are observed for all $A-B$ bonds. Especially for the N—N bonds in CH and C1—O1 in MC, the $R(\rho)$ from DZ (~1%) is more than four times smaller than that from SZ (4–5%). The $A-$H bond profiles, which are not included in Table 4, are only slightly improved, as the basis set for hydrogen has not been extended

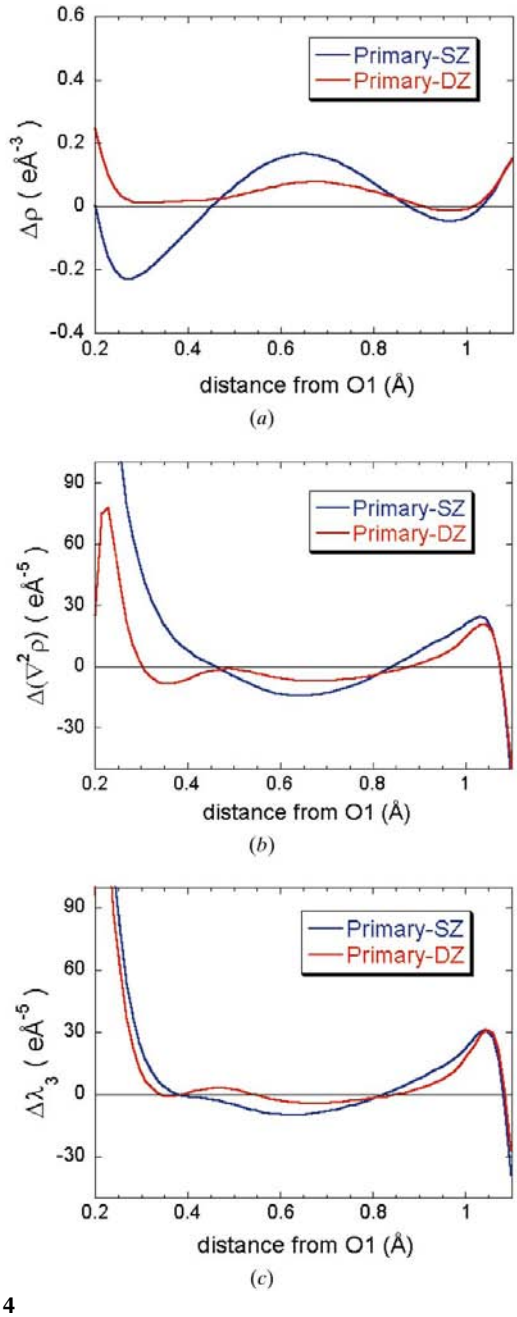

Figure 4
Differences in (*a*) ρ, (*b*) $\nabla^2\rho$ and (*c*) λ_3 profiles along the O1—C2 bond in methyl carbamate for the two models relative to the values based on the original wave function.

in this study. It is noticeable that the best $R(\rho)$ for different bonds is achieved for quite different combinations of n_l.

A remarkable consistency in n_l value (6–8) for the second deformation set is observed for the oxygen atoms, independent of their bonding environment. In the results of the KRMM (kappa-restricted multipole model), oxygen atoms showed a similar consistent behavior (Abramov *et al.*, 1999; Volkov, Abramov & Coppens, 2001). The values of n_l of the second deformation set for oxygen are correlated with the refined κ'' parameters. Thus, for $n_l = 8$, κ'' is between 1.5 and 1.7, while, for $n_l = 6$, κ'' is 1.2–1.3, which shows that the second deformation functions peak (at $n_l/\kappa''\zeta$) somewhere between 0.56 and 0.64 Å from the position of the oxygen nucleus. In some cases, the κ' parameters of the first set of deformation functions of the DZ refinement change significantly from the SZ values. For example, there is a dramatic change in the κ' value from 1.14–1.20 to 0.68–0.77 for the O1 and O2 oxygen atoms in MC and the O2 atom of GABA. This suggests that, if the DZ model is introduced in the refinement of experimental data, KRMM-type restrictions may have to be introduced in the DZ refinements.

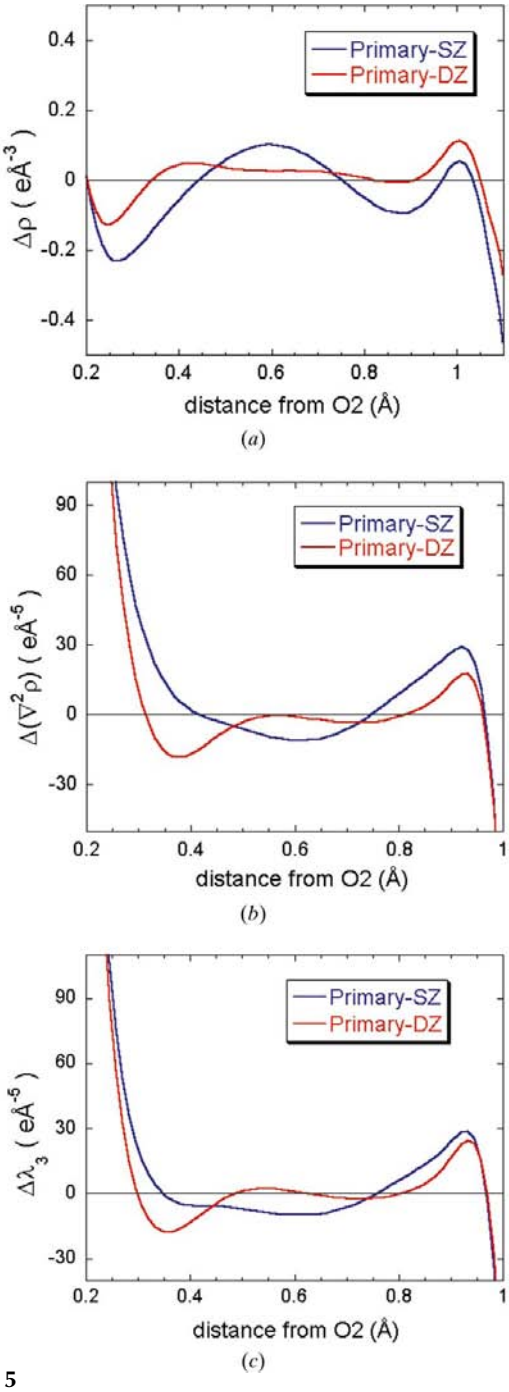

Figure 5
Differences in (*a*) ρ, (*b*) $\nabla^2\rho$ and (*c*) λ_3 profiles along the O2—C2 bond in methyl carbamate for the two models relative to the values based on the original wave function.

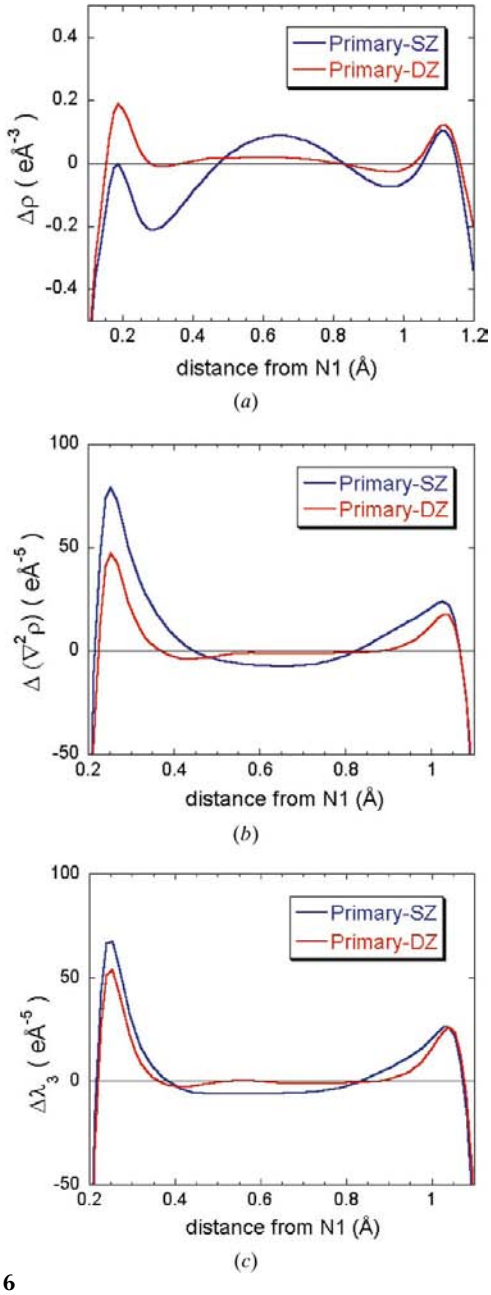

Figure 6
Differences in (*a*) ρ, (*b*) $\nabla^2\rho$ and (*c*) λ_3 profiles along the N1—C2 bond in methyl carbamate for the two models relative to the values based on the original wave function.

Table 4
Best profiles of ρ for different types of $A-B$ bonds in PNA, MC, CH and GABA from DZ refinements of PDFT structure factors with corresponding n_l, κ' and κ'' parameters.

		SZ			DZ								
						1st set		2nd deformation set					
			κ'			κ'		Atom A			Atom B		
	Bond $A-B$	$R(\rho)$ (%)	Atom A	Atom B	$R(\rho)$ (%)	Atom A	Atom B	$n_{1\ldots3}$	κ''	$n/\kappa''\zeta$†	$n_{1\ldots3}$	κ''	$n/\kappa''\zeta$†
N—O													
PNA	N2—O1	2.72	0.75	1.09	1.14	0.81	1.19	8	1.4	0.79	8	1.5	0.62
PNA	N2—O2	2.62	0.75	1.17	1.17	0.89	1.17	6	1.3	0.66	8	1.5	0.64
C—O													
MC	C2═O2	1.85	0.86	1.14	0.77	0.89	0.75	16	4.6	0.58	8	1.7	0.57
CH	C1═O1	1.84	0.87	1.17	0.64	0.88	1.02	18	5.5	0.55	8	1.7	0.56
MC	$C1_{methyl}-O1_{bridging}$	4.97	1.01	1.20	1.18	1.14	0.77	4	1.3	0.50	8	1.6	0.58
MC	$C2_{═O}-O1_{bridging}$	2.87	0.86	1.20	1.28	0.90	1.10	20	5.7	0.58	6	1.3	0.57
GABA	$C4_{carboxyl}-O1$	1.84	0.88	1.19	0.90	0.90	1.10	4	0.7	0.97	6	1.2	0.59
GABA	$C4_{carboxyl}-O2$	1.47	0.88	1.20	0.82	0.91	0.68	4	0.7	1.02	6	1.2	0.56
C—N													
PNA	$C1_{ar}-N1_{H\times2}$	1.93	0.82	0.93	0.81	0.85	1.30	8	1.6	0.82	4	0.9	0.65
PNA	$C4_{ar}-N2_{nitro}$	1.58	0.89	0.75	1.15	0.94	0.84	14	2.9	0.80	8	1.5	0.73
MC	$C2_{═O}-N1_{H\times2}$	2.28	0.86	0.95	0.67	0.89	0.82	20	5.8	0.57	8	1.9	0.59
CH	$C1_{═O}-N1_{H}$	2.13	0.87	1.01	0.76	0.85	0.90	8	2.6	0.52	18	3.8	0.65
CH	$C1_{═O}-N3_{H}$	2.04	0.87	1.03	0.74	0.85	0.92	18	5.3	0.57	14	3.0	0.65
GABA	$C1-N1_{H\times3}$	3.74	0.93	0.82	1.81	0.88	0.84	22	4.3	0.87	18	3.2	0.77
N—N													
CH	N1—N2	4.46	1.01	1.02	1.09	0.88	0.85	14	3.1	0.63	14‡	3.2	0.61
CH	N3—N4	4.64	1.03	0.99	0.96	0.91	0.86	16	3.5	0.63	16‡	3.6	0.61
C—C													
PNA	$C1-C2_{ar}$	1.34	0.82	0.93	0.72	0.98	0.79	6	1.3	0.78	6‡	1.2	0.82
PNA	$C2_{ar}-C3_{ar}$	1.20	0.93	0.89	0.60	0.91	0.99	4	0.8	0.80	4‡	0.8	0.78
PNA	$C3_{ar}-C4$	1.39	0.89	0.89	0.69	0.79	0.75	6	1.2	0.87	6‡	1.3	0.78
GABA	$C1_{primary}-C2_{primary}$	2.30	0.93	0.91	1.11	0.88	0.88	20	3.9	0.85	20‡	3.9	0.87
GABA	$C2_{primary}-C3_{primary}$	2.92	0.91	0.96	0.99	0.87	0.94	22	4.2	0.87	22‡	4.6	0.80
GABA	$C3_{primary}-C4_{carboxyl}$	1.70	0.96	0.88	0.86	0.89	0.90	4	0.7	0.95	4‡	0.7	0.97

† In ångstroms. ‡ Atom B has the same $n_{1\ldots3}$ as atom A because they are of the same type.

The nitrogen atoms can be separated into two groups based on n_l values of 4–8 and 14–18, respectively. The first group includes the N atoms of the NO_2 and NH_2 groups, where the latter is bonded to carbon. The second group consists of the nitrogen atoms of the NH_3 and NH groups and the nitrogen atom of the NH_2 group, when connected to another N atom. The second set of deformation functions peaks between 0.59 and 0.77 Å from the position of the nitrogen nucleus. As in the case of the oxygen atoms, some κ' parameters change significantly from SZ values. The largest change from 0.93 (SZ) to 1.30 (DZ) is found for the amino N atom in PNA.

Like the nitrogen atoms, the carbon atoms can be separated into two groups. The first group, with n_l = 16–22, consists of carbon atoms of the C═O and CH_2 groups, while the second, with n_l = 4–8, includes C atoms of CH_3 and CO_2 groups and aromatic C atoms. Although there are few exceptions because the same n_l was used for all carbon atoms in an individual DZ refinement, the trends are quite pronounced. The overall spread of the $n_l/\kappa''\zeta$ value for carbon is much larger than for the O and N atoms. The peaks of the second deformation functions range from 0.50 to 1.02 Å from the position of the carbon nuclei. At the extreme of this range, the second set of deformation functions on the carbon atom actually describes some of the charge density on the neighboring atom. The large variation of the value of $n_l/\kappa''\zeta$ for carbon is probably related to the fact that there is a relatively large variation in the bond lengths to the carbon atoms. The differences in κ' parameters between SZ and DZ are sometimes quite pronounced, though not as large as for the O and N atoms.

The results, listed in Table 4, suggest that, with the possible exception of oxygen, different n_l values may be needed for atoms of the same element in different bonding environments. Thus, the two carbon atoms in MC (C═O and C_{methyl}), as well as $C_{primary}$ and $C_{carboxyl}$ atoms in CH may have to be assigned different n_l values in the second deformation set. However, such a treatment will very probably require data with a larger $\sin\theta/\lambda$ cut-off value than used here.

Additional information can be extracted from Table 4.[1] For instance, there is a high correlation between κ'' and n_l values of the second deformation set, which means that the r_{max} values [equation (3)] show much less variation. However, radial functions with the same r_{max} but different n_l's differ by their half-width ($w_{1/2}$, width at half-maximum), with higher values of n_l corresponding to narrower functions. Thus the

[1] We are grateful to a referee for pointing this out.

Table 5
Net atomic charges derived from AIM analysis in methyl carbamate.

	PHF/6-31G**			PDFT(B3LYP)/6-31G**		
Atom	Primary density	SZ	DZ	Primary density	SZ	DZ
O1	−1.33	−1.16	−1.27	−1.14	−0.98	−1.09
O2	−1.48	−1.36	−1.44	−1.33	−1.19	−1.27
N1	−1.59	−1.17	−1.45	−1.40	−1.07	−1.23
C1	0.73	0.60	0.63	0.54	0.47	0.49
C2	2.59	2.22	2.55	2.23	1.86	2.13
H1	−0.01	−0.02	0.00	0.02	0.00	0.01
H2	−0.01	−0.02	0.00	0.01	−0.01	0.01
H3	−0.02	−0.03	−0.01	0.02	0.01	0.01
H4	0.56	0.48	0.50	0.53	0.47	0.48
H5	0.55	0.48	0.49	0.51	0.46	0.47

largest variation of $w_{1/2}$ occurs for carbon ($4 \leq n_l \leq 22$) and nitrogen ($4 \leq n_l \leq 18$) atoms, while the range of $w_{1/2}$ is much smaller for the oxygen atom ($6 \leq n_l \leq 8$). In general, the variation of $w_{1/2}$ can be related to the bonding environment of the particular atom type, as can the variation of the κ' parameter in the standard DZ multipole refinements (Volkov, Abramov & Coppens, 2001).

The better fit in ρ along the interatomic profiles from DZ multipole refinements should also produce better fits for the Laplacian and λ_3 (positive curvature along the bond). The remaining differences between the SZ and best DZ multipole results and the B3LYP-based profiles of ρ, the Laplacian $\nabla^2\rho$ and λ_3 for the $A-B$ bonds in methyl carbamate are plotted in Figs. 3–6. The profiles based on HF calculations show the same trends and are not shown here. A general improvement in ρ profiles and in Laplacian and λ_3 curves is obtained with DZ. The improvement for the Laplacian and λ_3 is especially pronounced for the N—C bonds. Profiles for PNA, CH and GABA, not shown here, show similar trends.

A better fit to the density should express itself in a superior reproduction of other physical properties. Considerable improvement is indeed observed in the AIM atomic charges and volumes for all molecules included in this study. Representative results for methyl carbamate are given in Tables 5 and 6, while those for the other molecules are listed in Tables S1–S6.[2] The improvement is most pronounced for the atomic charges, as is evident in Table 5, the agreement with the primary density being generally within 0.1 e, while discrepancies as large as 0.4 e are obtained for the SZ refinement. The changes in the charge correlate with the changes in atomic volume, as expected.

5. Solid-state molecular dipole moments

One of the prime interests in charge-density analysis concerns the effect of the crystal matrix on the charge distribution in a crystal. Evidence is accumulating that, as a result of induced polarization, dipole moments in crystals are significantly enhanced relative to isolated molecule values.

Comparison of AIM-derived molecular dipole moments (Table 7) from primary theoretical charge densities and those from multipole refinements shows some small improvements with the DZ model for PDFT calculations in PNA, MC and CH. The values obtained are different from the isolated molecule values, also listed in Table 7. In the case of PNA, the dipole moment change from 7.1–8.2 D for the isolated molecule to ~12 D, found experimentally (KRMM model), is confirmed by both DFT (11.8 D) and HF (11.2 D) periodic crystal calculations (Abramov *et al.*, 1999; Volkov, Gatti *et al.*, 2000). In methyl carbamate, the relative enhancement of the dipole moment is found to be quite large, from 2.5–2.8 D in the isolated molecule to 3.8–3.9 D in the neat crystal. On the other hand, the dipole-moment enhancements in carbonohydrazide (from 4.0–4.4 to 4.8–4.9 D) and γ-aminobutyric acid (from ~19 to ~20 D) are smaller than those of the other compounds studied here.

Table 6
Atomic volumes (in Å^3) in the methyl carbamate molecule from AIM analysis.

Calculated volume of the unit cell from cell parameters is 178.9 Å^3.

	PHF/6-31G**			PDFT(B3LYP)/6-31G**		
Atom	Primary density	SZ	DZ	Primary density	SZ	DZ
O1	16.5	16.7	16.8	16.1	16.2	16.4
O2	17.4	17.0	17.3	17.1	16.4	16.6
N1	19.5	18.0	18.8	18.6	17.5	17.8
C1	7.8	8.5	8.6	8.3	8.9	9.0
C2	2.7	3.1	2.6	3.8	4.1	3.8
H1	6.7	6.9	6.6	6.6	6.9	6.7
H2	7.1	7.0	6.7	7.0	7.0	6.8
H3	6.6	6.6	6.4	6.4	6.5	6.4
H4	2.6	2.9	2.8	2.9	3.1	3.0
H5	2.4	2.7	2.6	2.7	2.8	2.8
$V_{\rm AIM\ molecule}$ (Å^3)	89.3	89.4	89.3	89.4	89.3	89.3
$V_{\rm AIM\ unit\ cell}$ (Å^3)	178.6	178.7	178.6	178.9	178.6	178.6
$V_{\rm AIM\ unit\ cell}/V_{\rm calc}$ (%)	99.8	99.9	99.8	99.9	99.9	99.8

6. Conclusions

Our analysis confirms that significant discrepancies between topological parameters from experiment and theory are introduced by the limited flexibility of the single-zeta multipole model.

More diffuse values of the radial power coefficient $n_{1\ldots3}$ for non-H atoms (*i.e.* the 4, 4, 6 set) describe the topology of the charge density in the middle of the bond better than the conventional $n_{1\ldots3} = 2, 2, 3$ set, but give unacceptable deformation densities closer to the core region. The extension of the model with a second set of deformation functions for non-H atoms (the DZ model) with the same n_l for all multipolar functions for each atom type significantly improves topological properties such as the interatomic profiles of ρ, $\nabla^2\rho$ and λ_3, atomic charge and volumes, and molecular dipole moments. For C—N and, especially, C—C bonds, the topology

[2] Tables of net atomic charges and atomic volumes from AIM analysis of primary, and SZ and DZ multipole-refined PHF and PDFT charge densities for *p*-nitroaniline, carbonohydrazide and γ-aminobutyric acid are available from the IUCr electronic archives (Reference No. AU0237). Services for accessing these data are described at the back of the journal.

Table 7
AIM-derived theoretical molecular dipole moments (Debye) in PNA, MC, CH and GABA.

Components of the dipole moments are in the inertial coordinate system with the origin at the center of mass.

	$\|\mu\|$	μ_x	μ_y	μ_z
p-Nitroaniline				
Isolated molecule in crystal geometry:				
HF/6-311G**	8.2	8.2	0.0	0.1
BPW91/6-311G**	8.0	8.0	0.0	0.1
MP2/6-311G**	7.1	7.1	0.0	0.1
PHF/6-31G** (crystal):				
Primary density†	11.2	11.2	0.2	0.0
SZ ($n_{1\ldots3}$ = 2, 2, 3)‡	11.3	11.3	0.4	0.1
SZ ($n_{1\ldots3}$ = 4, 4, 6)‡	11.4	11.4	0.4	0.1
DZ§	11.2	11.2	0.3	0.1
PDFT(PBPW91)/6-31G** (crystal):				
Primary density†	11.8	11.8	0.2	−0.1
SZ ($n_{1\ldots3}$ = 2, 2, 3)‡	11.3	11.5	0.3	0.2
DZ§	11.8	11.8	0.3	−0.1
Methyl carbamate				
Isolated molecule in crystal geometry:				
HF/6-311++G**	2.80	0.36	−2.77	−0.12
B3LYP/6-311++G**	2.61	0.42	−2.58	−0.11
MP2/6-311++G**	2.46	0.37	−2.43	−0.11
PHF/6-31G** (crystal):				
Primary density†	3.93	0.59	−3.87	−0.28
SZ ($n_{1\ldots3}$ = 2, 2, 3)‡	3.90	1.66	−3.53	−0.14
DZ§	3.96	1.07	−3.81	−0.18
PB3LYP/6-31G** (crystal):				
Primary density†	3.83	0.79	−3.73	−0.28
SZ ($n_{1\ldots3}$ = 2, 2, 3)‡	3.69	1.68	−3.29	−0.12
DZ§	3.89	1.51	−3.58	−0.20
Carbonohydrazide				
Isolated molecule in crystal geometry:				
HF/6-311++G**	4.41	−3.98	−1.79	0.65
B3LYP/6-311++G**	4.13	−3.77	−1.58	0.64
MP2/6-311++G**	4.02	−3.70	−1.44	0.65
PHF/6-31G** (crystal):				
Primary density†	5.37	−4.87	−2.10	0.85
SZ ($n_{1\ldots3}$ = 2, 2, 3)‡	4.76	−4.41	−1.57	0.87
DZ§	4.85	−4.63	−1.08	0.97
PDFT(B3LYP)/6-31G** (crystal):				
Primary density†	4.88	−4.40	−1.95	0.84
SZ ($n_{1\ldots3}$ = 2, 2, 3)‡	4.33	−3.98	−1.53	0.75
DZ§	4.81	−4.36	−1.86	0.82
γ-Aminobutyric acid				
Isolated molecule in crystal geometry:				
HF/6-311++G**	20.38	20.24	2.40	0.15
B3LYP/6-311++G**	19.01	18.90	2.03	0.22
MP2/6-311G**	19.03	18.97	1.61	0.26
PHF/6-31G** (crystal):				
Primary density†	21.72	21.57	2.54	−0.14
SZ ($n_{1\ldots3}$ = 2, 2, 3)‡	21.43	21.36	1.67	−0.32
DZ§	21.28	21.21	1.69	−0.20
PDFT(B3LYP)/6-31G** (crystal):				
Primary density†	20.23	20.12	2.10	−0.20
SZ ($n_{1\ldots3}$ = 2, 2, 3)‡	19.22	19.18	1.29	−0.24
DZ§	19.10	19.06	1.21	−0.14

† AIM analysis of primary density. ‡ SZ multipole refinement of theoretical structure factors. § DZ multipole refinement of theoretical structure factors.

of the charge density obtained with the DZ model is in very good agreement with the primary density but some discrepancies remain for most polar bonds such as N—O and C—O. A further improvement can probably be obtained by use of separate n_l values for the second set of deformation functions for each atom in a specific bonding environment or by using different n_l values for different l's for a specific atom type. A further extension would involve triple-zeta multipole basis sets with different values of n_l for second and third sets of deformation functions. However, all such schemes would probably require data sets with higher than 1.1 Å^{-1} resolution.

Finally, application of the DZ model in refinement of experimental data will require structure factors of exceptional accuracy. With the continued improvement in experimental capabilities, such data may well become available in the not too distant future. Examination of extended models as presented here will provide guidance for future applications.

The authors would like to thank Dr Koritsanszky for modifications in the *XD* code and a referee for valuable comments and suggestions. Support of this work by the National Science Foundation (CHE9981864) and the US Department of Energy (DE-FG02-86ER45231) is gratefully acknowledged. Theoretical calculations were performed on a 128-processor Silicon Graphics Origin2000 supercomputer and a 64-node Beowulf SUN Ultra5 cluster at the Center for Computational Research at SUNY at Buffalo, which is supported by a grant (DBI9871132) from the National Science Foundation.

References

Abramov, Yu. A., Volkov, A. & Coppens, P. (1999). *Chem. Phys. Lett.* **311**, 81–86.
Abramov, Yu. A., Volkov, A., Wu, G. & Coppens, P. (2000). *J. Phys. Chem.* A**104**, 2183–2188.
Bader, R. F. W. (1990). *Atoms in Molecules: a Quantum Theory*. Oxford: Clarendon Press.
Becke, A. D. (1988). *Phys. Rev. A*, **38**, 3098–3100.
Becke, A. D. (1993). *J. Chem. Phys.* **98**, 5648–5652.
Chandler, G. S. & Spackman, M. A. (1982). *Acta Cryst.* A**38**, 225–239.
Chandler, G. S., Spackman, M. A. & Varghese, J. N. (1980). *Acta Cryst.* A**36**, 657–669.
Clark, T., Chandrasekhar, J. & Schleyer, P. v. R. (1983). *J. Comput. Chem.* **4**, 294–301.
Clementi, E. & Roetti, C. (1974). *At. Data Nucl. Data Tables*, **14**, 177–478.
Coppens, P. (1997). *X-ray Charge Densities and Chemical Bonding*. New York: Oxford University Press.
Frisch, M. J., Trucks, G. W., Schlegel, H. B., Gill, P. M., Johnson, B. G., Robb, M. A., Cheeseman, J. R., Keith, T., Petersson, G. A., Montgomery, J. A., Raghavachari, K., Al-Laham, M. A., Zakrzewski, V. G., Ortiz, J. V., Foresman, J. B., Cioslowski, J., Stefanov, B. B., Nanayakkara, A., Challacombe, M., Peng, C. Y., Ayala, P. Y., Chen, W., Wong, M. W., Andres, J. L., Replogle, E. S., Gomperts, R., Martin, R. L., Fox, D. J., Binkley, J. S., Defrees, D. J., Baker, J., Stewart, J. P., Head-Gordon, M., Gonzalez, C. & Pople, J. A. (1995). *Gaussian94, Revision E.2.* Gaussian Inc., Pittsburgh, PA, USA.
Gatti, C. (1999). *TOPOND98 Users Manual.* CNR-CSRSRC, Milano, Italy.
Hansen, N. K. & Coppens, P. (1978). *Acta Cryst.* A**34**, 909–921.
Hariharan, P. C. & Pople, J. A. (1973). *Theor. Chim. Acta*, **28**, 213–222.
International Tables for Crystallography (1992). Vol. C, edited by A. J. C. Wilson. Dordrecht: Kluwer Academic Publishers.

Iversen, B. B., Larsen, F. K., Figgis, B. N. & Reynolds, P. A. (1997). *J. Chem. Soc. Dalton Trans.* pp. 2227–2240.
Jeffrey, G. A., Ruble, J. R., Nannio, R. G., Turano, A. M. & Yates, J. H. (1985). *Acta Cryst.* B**41**, 354–361.
Koritsanszky, T. (2000). Unpublished.
Koritsanszky, T., Howard, S., Su, Z., Mallinson, P. R., Richter, T. & Hansen, N. K. (1997). *XD – a Computer Program Package for Multipole Refinement and Analysis of Electron Densities from Diffraction Data.* Free University of Berlin, Berlin, Germany.
Krishnan, R., Binkley, J. S., Seeger, R. & Pople, J. A. (1980). *J. Chem. Phys.* **72**, 650.
Lee, C., Yang, W. & Parr, R. G. (1988). *Phys. Rev. B*, **37**, 785–789.
Møller, C. & Plesset, M. S. (1934). *Phys. Rev.* **56**, 618.
Monkhorst, H. J. & Pack, J. D. (1976). *Phys. Rev. B*, **13**, 5188.
Moss, G. R., Souhassou, M., Blessing, R. H., Espinosa, E. & Lecomte, C. (1995). *Acta Cryst.* B**51**, 650.
Perdew, J. P. & Wang, Y. (1992). *Phys. Rev. B*, **45**, 13244.
Pérès, N., Boukhris, A., Souhassou, M., Gavoille, G. & Lecomte, C. (1999). *Acta Cryst.* A**55**, 1038–1048.
Saunders, V. R., Dovesi, R., Roetti, C., Causà, M., Harrison, N. M., Orlando, R. & Zicovich-Wilson, C. M. (1998). *CRYSTAL98 Users Manual.* University of Torino, Italy.
Sepehrnia, B., Ruble, J. R. & Jeffrey, G. A. (1987). *Acta Cryst.* C**43**, 249.
Stewart, R. F. J. (1969). *J. Chem. Phys.* **51**, 4569–4577.
Stewart, R. F. (1976). *Acta Cryst.* A**32**, 565–574.
Swaminathan, S., Craven, B. M., Spackman, M. A. & Stewart, R. F. (1984). *Acta Cryst.* B**40**, 398–404.
Volkov, A., Abramov, Y. & Coppens, P. (2001). *Acta Cryst.* A**57**, 272–282.
Volkov, A., Abramov, Y., Coppens, P. & Gatti, C. (2000). *Acta Cryst.* A**56**, 332–339.
Volkov, A., Blaha, P., Coppens, P. & Schwartz, K. (2001). Unpublished results.
Volkov, A., Gatti, C., Abramov, Y. & Coppens, P. (2000). *Acta Cryst.* A**56**, 252–258.
Weber, H.-P., Craven, B. M. & McMullan, R. K. (1983). *Acta Cryst.* B**39**, 360–366.